Hierarchical Extraction and Verification of Symmetry Constraints for Analog Layout Automation[*]

Sambuddha Bhattacharya, Nuttorn Jangkrajarng, Roy Hartono and C-J. Richard Shi

Department of Electrical Engineering, University of Washington
Seattle, WA 98195, USA
{sbb, njangkra, rhartono, shi}@ee.washington.edu

Abstract - Device matching and layout symmetry are of utmost importance to high performance analog and RF circuits. In this paper, we present HiLSD, the first CAD tool for the automatic detection of layout symmetry between two or more devices in a hierarchical manner. HiLSD first extracts the circuit structure from the layout, then applies an efficient pattern-matching algorithm to find all the subcircuits automatically, and finally detects layout symmetry on the portion of the layout that corresponds to extracted subcircuit instances. On a set of practical analog layouts, HiLSD is demonstrated to be much more efficient than direct symmetry detection on a flattened layout. Results from applying HiLSD to automatic analog layout retargeting for technology migration and new specifications are also described.

I Introduction

Variations in the process poly-silicon etch rate, dopant concentration and gradients in temperature, stress and oxide thickness affect the threshold voltage, mobility and current-factors in MOS transistors [1]. These effects on the device characteristics introduce mismatches in transistors that are designed to behave identically. Such mismatches drastically affect analog circuit performance leading to DC offsets, finite even-order distortion and lower common-mode rejection [2]. Symmetric layout of matched transistors alleviates the effects of mismatch in analog/RF circuits.

Device matching and symmetry along with floorplanning, placement and parasitic-driven wiring considerations pose considerable challenge to the automation of analog/RF layouts [2][3]. Over the years, macro-cell based automated placement and routing methodologies have been proposed for analog circuits [4][5]. These layout automation schemes, despite their effectiveness and generality, often fail to incorporate the expertise of the layout designer and are seldom accepted in the industry.

For technology migration and changes in performance specification of analog/RF circuits, a layout reuse methodology promises to be a viable alternative. Such methodologies for analog layout retargeting through layout-template creation by a procedural-language or graphical-user-interface have been proposed in [6][7]. Unfortunately, creation of such templates demands substantial effort from the user. In contrast, [8] recently proposed an automatic layout retargeting methodology for analog circuits, in which an already fined-tuned layout is used to automatically create a *symbolic structural template* incorporating floorplan, symmetry and device/wiring alignment information. The new device sizes under retargeting are imposed on the template and the output layout is generated by layout compaction with symmetry constraints [9].

In [8], the axes of symmetry obtained from the existing layout are used as constraints in the structural template. As will be elaborated later, the complexity of such layout retargeting methods is strongly dependent on the number of symmetry axes and corresponding constraints. Therefore, the efficient detection of layout symmetry represents an essential step for the analog layout retargeting process.

An algorithm was proposed in [10] for the detection of layout symmetry. Under this scheme, symmetry detection is accomplished by scanning the entire layout for all horizontally or vertically aligned equi-sized transistors. Unfortunately, this leads to the detection of all unintended axes of symmetry that reside in the layout. Such redundant axes over-constrain the structural template thereby rendering the layout retargeting process computationally expensive.

In this paper, we present a CAD tool, HiLSD (**Hi**erarchical **L**ayout **S**ymmetry **D**etector), which automatically detects layout symmetry based on circuit hierarchy. First, the layout is extracted for the circuit netlist. Then, the circuit hierarchy is established from this flat netlist based on a library of subcircuits that contain device matching information. The detection of the axes of symmetry in the layout is then initiated from the hierarchical netlist. By triggering symmetry detection from the circuit-specific information, HiLSD significantly curtails the search-space and ignores all unintended axes of symmetry that reside in the layout. HiLSD generates a very concise set of symmetry constraints for the automatic layout retargeting process.

Furthermore, in a typical design company, layout and circuit designs are seldom accomplished by the same personnel. For the conscientious circuit designer, HiLSD provides an interactive mode of layout symmetry verification from its graphical user interface.

This paper is organized as follows. Section II discusses the background and the motivation for this work. Section III illustrates the methodology employed for symmetry detection in HiLSD. Section IV explains the process of netlist and hierarchy extraction. Section V describes the actual detection of symmetry from the layout. Section VI presents the experimental results of HiLSD and its application in analog layout automation. Section VII concludes the paper.

II. Background and Motivation

A. Background

A MOS transistor in a layout is defined as an overlap between two rectangles in the *poly-silicon* and *diffusion* mask layers and has three terminals, viz., the gate terminal in the poly-silicon layer and the source and drain terminals in the diffusion layer. Good matching between any pair of transistors is established by laying out the transistors symmetrically. Two transistors are deemed to be symmetric if their layouts are geometric mirror images of each other. As illustrated in Fig. 1, this implies equi-sized channel, drain and source regions, identical orientation and close proximity of the two transistors. For large or multi-fingered transistors, simple geometric mirroring may not establish acceptable matching due to the thermal and process gradients. Such transistor-pairs are often laid-out cross-coupled in one dimension, Fig. 2, or in the two-dimensional cross-coupled form of Fig. 3 also known as the common-centroid layout.
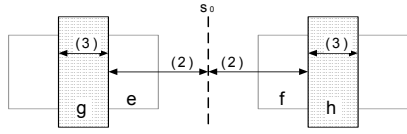
Fig. 1: A simplified layout of two symmetric transistors. Only diffusion and the poly-silicon (dotted) layers are shown. The symmetry axis is denoted by 's_0'.
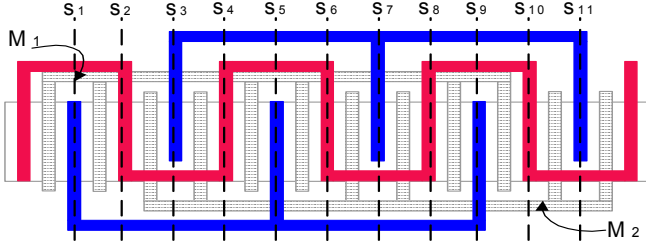

Fig. 2: A one-dimensional cross-coupled symmetric transistor pair. The rectangles with dotted patterns represent the poly-silicon layer.
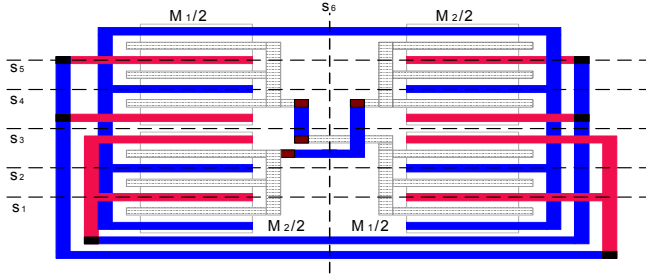

Fig. 3: A common-centroid layout of a symmetric transistor pair. Rectangles with dotted pattern represent the poly-silicon layer.

The layout symmetry detection algorithm presented in [10], henceforth called Direct Layout Symmetry Detection (DLSD), relies on scanning the entire layout for symmetric transistors. First, the nets and transistors in the layout are identified and all transistors are stored in a queue sorted by their bottom-edges. Devices connected by a net and with same ordinate of bottom-edges are then pairwise compared for the existence of geometric mirror images. After detection of all symmetric transistor-pairs, all axes of symmetry with same abscissa or ordinate are merged into a single axis. Under this scheme, the layout of Fig. 2 has eleven axes of symmetry marked by the axes s_1 to s_{11} and sixty-six (selecting 2 from 12) matched transistor pairs. The layout in Fig. 3 has six axes of symmetry as indicated by the axes s_1 to s_6 and thirty matched transistor pairs.

B. Motivation: Analog Layout Retargeting

The automatic layout retargeting methodology [8] provides an efficient way of reusing existing fine-tuned analog layouts over changes in technology and design specifications. The re-targeting tool reads in a hand-crafted analog layout, the source and target technology-dependent design rules and automatically creates a symbolic structural template. By imposing the new device sizes pertaining to new specifications on the template, the tool generates a target layout that maintains all the designer expertise embedded in the source layout. The internal flow diagram of the retargeting tool is shown in Fig. 4.

The retargeting tool-suite consists of a template extractor and a layout generator. The symbolic template, extracted from the source layout by the template extractor, comprises the design-rules, connectivity and symmetry constraints. The following equations represent the symmetry constraints generated for the layout of Fig. 1.

$$(e_{top} - f_{top}) = (e_{bottom} - f_{bottom}) = 0 \qquad (1)$$

$$(s_0 - g_{right}) - (h_{left} - s_0) = 0 \qquad (2)$$

$$(g_{right} - g_{left}) - (h_{right} - h_{left}) = 0 \qquad (3)$$

Here, s_0 represents the symmetry axis and all other variables represent the edges of the rectangles. Eq. (1) enforces the alignment at the same ordinate and the equality of the widths of the transistors. The equidistance of the transistors from the symmetry axis is imposed by Eq. (2). The equality of the gate-lengths is enforced by Eq. (3).
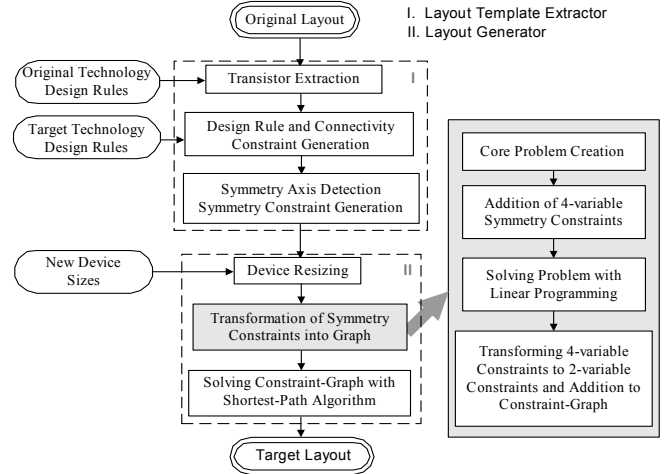

Fig. 4: Internal Flow for template-based layout retargeting.

The problem of the generation of a new layout from the symbolic template reduces to solving a constrained *symbolic compaction* problem [13]. The layout generator tool solves this compaction problem after imposing new device sizes on the symbolic template. While *linear programming* (LP) [14] can be employed to solve this problem, it is computationally intensive and therefore prohibitive for large problems. Therefore, the compaction problem is solved by a combination of linear programming and graph-based shortest-path algorithm [9].

The constraint equations, therefore, need to be transformed into a constraint-graph $G(V,E)$. While the design rule and connectivity constraints can be directly mapped to the constraint-graph, the transformation of the three or four variable symmetry constraints in Eqs. (2) and (3) is rather complex. The steps in the transformation of the symmetry-dictated constraint equations to the graph form have been magnified on the right in Fig. 4. First, the graph $G(V,E)$ obtained from the design rule constraints is reduced to a smaller graph called *core-graph* $G_1(V_1,E_1)$ where $V_1 \subset V$ and $V_1 = \{v_i \mid v_i$ corresponds to the variables in the equi-distance constraint-equations} [9]. The edges of the core-graph are obtained by applying the shortest path algorithm on the main constraint graph $G(V,E)$. A directed edge $e(v_i,v_j)$ is added between the pair of vertices in G_1 if there exists a shortest path between the corresponding vertices in $G(V,E)$.

The LP-compatible equations are generated from the core-graph G_1. The solution of these equations transforms the equidistance constraints in a form that can be directly incorporated into the main constraint graph G. For example, Eq. (2) is transformed into a form

$$s_0 - g_{right} = h_{left} - s_0 = b \qquad (4)$$

where b is a constant. Once all the three and four-variable constraint-equations are transformed and added into the main

constraint-graph, the symbolic compaction problem is solved using the shortest-path algorithm.

Thus, each symmetry axis introduces numerous variables and necessitates multiple transformations of the constraint-graph into the core-graph [9]. A large number of symmetry axes render the process very computation intensive. Also, as we found during our retargeting experiments, too many redundant symmetry constraints may even render the problem unsolvable. Clearly, reducing the number of symmetry axes and avoiding all redundant constraints is essential for efficient layout retargeting.

III. Hierarchical Symmetry Detection Flow

As discussed in Section II, reduction of symmetry constraints and avoidance of unintentional symmetry is a prime requirement for successful and efficient layout retargeting. The method proposed in this work is based on layout proximity based clustering of netlist and extraction of hierarchy information from the circuit. This is illustrated in Fig. 5.
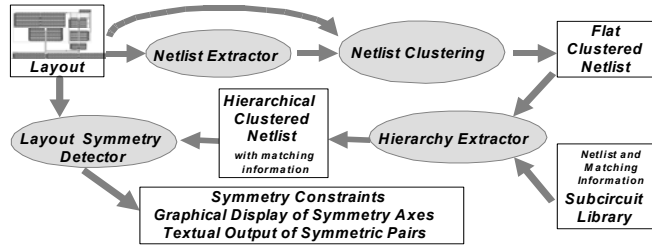

Fig. 5: Hierarchical Symmetry Detection Methodology. The oval blocks are modules of HiLSD.

First, the Netlist Extractor generates the circuit netlist from the layout information. The netlist is then clustered into groups based on physical proximity in the layout. A designer-provided library consists of the netlists of the building blocks, and matching and symmetry information of individual devices. The subcircuits in the library can be any commonly used analog circuit like differential pair, current mirror or larger hierarchical blocks like comparators, operational amplifiers etc. For simple building blocks such as differential pair and current mirror, the matching information is implicitly embedded in the library, whereas for larger complex blocks like operational amplifiers, explicit matching information may be input by the designer. The Hierarchy Extractor identifies all instances of the subcircuit in the main netlist. During this Subcircuit mapping, a complete list of essential and intended matched transistor pairs is created. The detection of symmetric transistors in the layout is initiated from the list obtained after Subcircuit mapping.

Table 1: Outline of the HiLSD algorithm.

```
HierarchicalLayoutSymmetryDetection
begin
    detectNetsTransistors
    clusterTransistors
    for each  s ∈ L    // s = subcircuit, L = Library
        mapSubcircuits
    end for
    detectLayoutSymmetry
end
```

Table 1 shows all the steps in the hierarchical symmetry detection algorithm. The procedures *detectNetsTransistors* extracts the netlist from the layout and *clusterTransistors* groups transistors that are physically contiguous in the layout. The routine *mapSubCircuits* inside the loop identifies all instances of the library subcircuits and

maps them to the layout data-structure. This mapping process identifies all the matched transistors that are meant to be symmetric in the layout. Finally, the detection of layout symmetry and generation of constraints are accomplished in the routine *detectLayoutSymmetry*. Each of these processes is explained in detail in Sections IV and V.

IV. Netlist, Cluster and Hierarchy Extraction

A. Netlist Extraction

A transistor with a single rectangle each for its gate, source and drain terminals is henceforth called a *unit transistor*. A net is defined as an electrical connection between the terminals of transistors or external ports.

The layout representation and netlist extraction schemes are adopted from the *Magic* VLSI layout system [11]. Unit transistors are detected by an efficient search for overlaps between the poly-silicon and the diffusion layers. The netlist database stores the location, size, orientation and terminal information for each unit transistor. Once the transistors are extracted, a simple recursive algorithm detects the nets from the layout using the terminals of the transistors as the starting points.

B. Proximity Based Netlist Clustering

The netlist clustering process is especially important as it reduces the number of symmetry axes for multi-fingered transistors. In the layout, each multi-fingered transistor M contains multiple contiguous elements C, where each contiguous element consists of physically contiguous unit transistors T. The clustering scheme partitions the netlist based on the manner in which the transistors are laid out.

The netlist, which at the end of extraction comprised of the set of unit transistors T^S and the set of nets N^S, now consists of the same set of nets N^S and the set of multi-fingered transistors M^S defined as $\{M \,|\, \forall M \,\exists$ a unique $\{G_M, S_M, D_M\} \subset N^S\}$ where $\{G_M, S_M, D_M\}$ is the set of the gate, source and drain nets of the multi-fingered transistor M. Each multi-fingered transistor M is a set of physically contiguous elements C^S i.e., $C \in M$ or in other words, $M = C^S = \{C\}$. And each contiguous elements is defined as $C = \{T \,|\, T \in T^S, \forall T \,\{G_T, S_T, D_T\} = \{G_M, S_M, D_M\}, \text{ and } \forall T \in C$ *are physically contiguous*$\}$. For the one-dimensional cross-coupled symmetric pair of Fig. 2, each multi-fingered transistor has three contiguous sets of two unit transistors each. In Fig. 3, each multi-fingered transistor has two contiguous sets of three unit transistors each.

Table 2: Algorithm for netlist partitioning.

```
clusterTransistors
begin
    for each  N ∈ N^S       // N^S  is the set of nets
        // G_T , S_T , D_T are gate,source,drain nets of transistor T
        for each  T ∈ T^S | N ∈ { G_T , S_T , D_T }
            M  = checkCreateMFT ( G_T , S_T , D_T )
            X  = checkCreateContiguous ( C^S , T )  // M = C^S = {C}
            insertSorted ( T , X )   // doubly sorted w.r.t.  x, y co-ordinates
        end for
    end for
end
```

The *clusterTransistors* procedure in Table 2 presents the algorithm for partitioning the netlist. Each multi-fingered transistor is stored in a hashtable with hash *key* formed by the drain, gate and

source nodes. For each unit transistor T connected to a net N, a new multi-fingered transistor M is created if it does not already exist in the hashtable. This is accomplished by a call to the routine *checkCreateMFT*. The routine *checkCreateContiguous* then checks if the unit transistor T is aligned with one of the contiguous elements in M. If T is not physically contiguous with any $C \in M$, a new contiguous element is created. In either case, the routine *insertSorted* inserts T into a list of unit transistors of the corresponding contiguous element. This list of transistors in a contiguous element is doubly sorted with respect to the x and y coordinates.

C. *Hierarchy Extraction*

The designer-intended transistor-matching information is embedded in the subcircuits in the library. Identifying instances of these commonly used subcircuits in the main netlist maps the non-redundant matching information to the devices in the layout. This is accomplished by an efficient subgraph isomorphism algorithm [12] in the *mapSubcircuits* routine of Table 1.

First, both the subcircuit and the main circuit are implicitly partitioned by an iterative labeling algorithm to reduce the search space. This identifies a set of nodes in the main circuit and a single node, called a *key* node, in the subcircuit. The set of nodes in the main circuit obtained by this iterative labeling algorithm are potential start-points for checking a pattern match with the subcircuit. From each potential node in the main circuit and the key node in the subcircuit, another labeling algorithm accomplishes detection of an isomorphism with the subcircuits graph.

V. Layout Symmetry Detection

The hierarchy extraction process generates a subcircuit-based netlist. From the subcircuit-based netlist, a list of designer-intended non-redundant matched multi-fingered transistor pairs is created. The layout symmetry detection scheme identifies if each pair of these multi-fingered transistors is actually laid out symmetrically. The process also generates the corresponding constraints for the ensuing compaction step in layout automation[8].

The algorithm for layout symmetry detection is shown in Table 3. For each transistor pair intended to be matched, the *detectTopology* routine identifies the pair's layout topology by traversing through the list of contiguous elements. Based on the topology, the unit transistors are inserted into two or four sorted lists. Thus, for the common-centroid topology of Fig. 3, the six unit transistors in the top and bottom halves of the transistors M_1 and M_2 respectively are collected into a list L_L. The bottom and top halves of M_1 and M_2 are collected into another list L_R. The unit transistors in L_L and L_R are then pairwise compared in the *checkSymmetry* routine to detect the vertical axis of symmetry, s_6, and generate the corresponding constraints. For the horizontal symmetry axis s_3, the bottom halves of both M_1 and M_2 are collected into a list L_B, and the top halves are collected into a list L_T and pairwise compared. For the layout of Fig. 2, six unit transistors are inserted into each list L_L and L_R and a single axis of symmetry s_6 is detected. Prior co-ordinate based double sorting of the unit transistors in each multi-fingered transistor ensures that pairwise comparison can detect axes of symmetry.

VI. Results

A. *Symmetry Detection Experiments*

The HiLSD program was employed to detect symmetry in various analog/RF layouts and generate constraints for the layout retargeting methodology [8] illustrated in Fig. 4. Table 4 compares the symmetry detection data for HiLSD with the DLSD method presented in [10]. Various symmetry topologies were employed on the different layouts. The differential amplifier, the latched comparator and the 4:1 comparator used symmetric transistors with minimal multi-fingered structures. The voltage-controlled oscillator was laid out with extensive multi-fingered symmetric transistors. The two-stage and folded-cascode operational amplifiers utilized multi-fingered interleaved and common-centroid symmetry topologies. And the 5-bit flash analog-to-digital converter consisted of 31 instances of a latched-comparator laid out in an array of 8x4.

For each method, the number of symmetry axes detected, the number of symmetric transistor pairs, and the number of constraints due-to-symmetry are reported. The DLSD method extracted a large number of redundant symmetry axes. As it detected symmetry between every pair of unit transistors in each multi-fingered transistor, a large number of axes were observed for the two-stage operational amplifier and the voltage-controlled oscillator circuits. For the array structure of the comparator blocks in the 5-bit analog-to-digital converter, the DLSD method detected symmetry for every transistor in one comparator cell to every transistor in another comparator cell in the same row and column. These redundant constraints not only slowed down the compaction steps in layout retargeting, but also rendered the problem unsolvable in some cases.

Table 3: Algorithm for symmetry detection.

```
detectLayoutSymmetry
begin
   // ListSym = { (M_i , M_j) | M_i and M_j are intended matched pair }
   for each ( M_i , M_j ) ∈ ListSym
       topology = detectTopology ( M_i , M_j )
       if ( topology == common_centroid ) then
           L_L = insertToList ( M_i , M_j , left )
           L_R = insertToList ( M_i , M_j , right )
           L_B = insertToList ( M_i , M_j , bottom )
           L_T = insertToList ( M_i , M_j , top )
           checkSymmetry ( L_L , L_R )
           checkSymmetry ( L_B , L_T )
       else if ( topology == horizontal_interleaving ) then
           L_L = insertToList ( M_i , M_j , left )
           L_R = insertToList ( M_i , M_j , right )
           checkSymmetry ( L_L , L_R )
       else if ( topology == vertical_interleaving ) then
           L_B = insertToList ( M_i , M_j , bottom )
           L_T = insertToList ( M_i , M_j , top )
           checkSymmetry ( L_B , L_T )
       else        // simple transistor layout
           checkSymmetry ( M_i , M_j )
       end if
   end for
end
```

We compare the scaling of the symmetry detection by the two methods with arrays of comparators. Fig. 6 shows the number of symmetric transistor pairs detected by DLSD and HiLSD as the number of comparators is scaled. The y-axis is in logarithmic scale. The graph shows that DLSD detects a huge number of redundant symmetry axes.

| Circuits	# Multi-Fingered Transistors	# Unit Transistors	Design Rule Constraints	DLSD			HiLSD		
				Symmetry Axes	Transistor Pairs	Symmetry Constraints	Symmetry Axes	Transistor Pairs	Symmetry Constraints
Differential Amplifier	5	5	1,602	1	2	18	1	2	18
Latched Comparator	15	20	8,639	10	19	132	2	6	42
2-stage Opamp	9	48	5,902	69	262	1,578	2	12	78
Folded Cascode Opamp	14	43	8,352	29	173	1,206	6	20	168
4:1 Comparator	20	32	26,182	26	166	1,026	3	13	78
VCO	16	198	645,986	680	5,525	33,156	4	362	2,178
5-bit Flash ADC	435	590	320,937	261	6,218	4,193	12	186	1,302

B. *Automatic Analog Layout Retargeting with HiLSD*

We performed experiments on analog layout retargeting [8] to a new technology and specifications based on the hierarchical and direct symmetry detection methods. Fig. 7 shows a comparator layout in TSMC 0.25um CMOS process.   This layout was retargeted under new specifications to the TSMC 0.18um CMOS technology using both DLSD and HiLSD based symmetry detection.

The symmetry constraints generated by the two methods were passed onto the resizing tool. Table 5 shows the number of symmetry axes, transistor pairs, symmetry constraints, and user runtime for the resizing schemes under the two methods. The retargeted layout obtained by using HiLSD for symmetry detection is shown in Fig. 8. The retargeted layout under this preserved all the required matching considerations, while incorporating a lesser number of symmetry constraints. The circuit performance of the latched-comparator in the two technologies achieved by these methods is reported in Table 6.
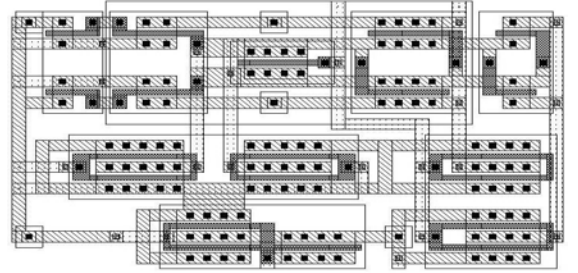

Fig. 7: Comparator Layout in TSMC 0.25um technology.
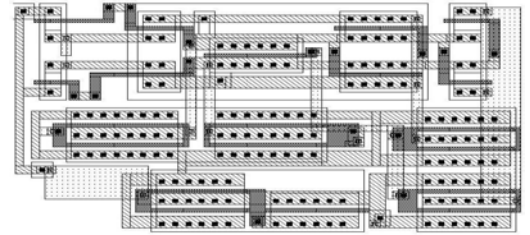
Fig. 8: Retargeted Layout of comparator in TSMC 0.18um
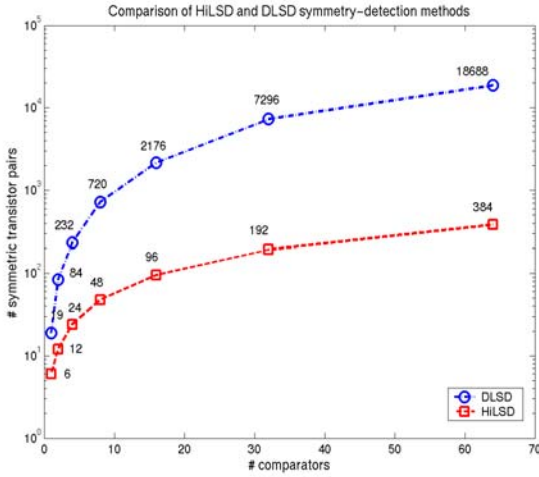
Fig. 6: Comparison of HiLSD and DLSD symmetry detection for array of comparators. X-axis represents number of comparators in the array. Y-axis denotes number of symmetric transistor pairs (Log scale).

The analog comparator section of the 5-bit flash analog-to-digital converter was constructed by placing 31 units of the latched-comparator into an 8x4 array. Each unit comparator was aligned   and   matched with other units in the same row and column. For any unit comparator in the section, another comparator corresponding to its preceding or following bit was positioned next to each other to minimize the mismatch.   The layout of the comparator section of the ADC in TSMC 0.25um CMOS technology is shown in Fig. 9.
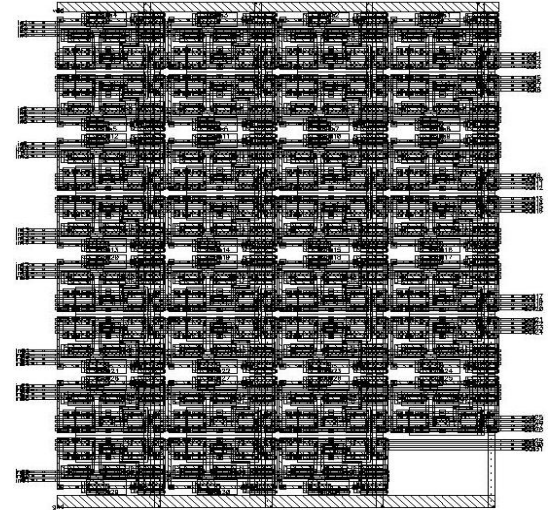
Fig. 9: Comparator block of a 5-bit flash ADC in TSMC 0.25um.

The flash analog-to-digital converter was retargeted to the TSMC 0.18um CMOS process; first with the symmetry information obtained from DLSD method and then with the HiLSD algorithm. DLSD detected 6,218 symmetric transistor pairs in the layout, while the HiLSD method identified only 186 symmetric pairs.   This huge difference in detected symmetric pairs is due to the redundant symmetric pairs from the transistors on different unit   comparators

Table 5: Comparison between layout retargeting with DLSD and HiLSD symmetry detection schemes.

Design	Latched Comparator		5-bit Flash Analog-to-Digital Converter	
Symmetry Detection Method	DLSD	HiLSD	DLSD	HiLSD
Multi-fingered Transistors	15	15	435	435
Unit Transistors	20	20	590	590
Design Rule Constraints	8,639	8,639	320,937	320,937
Symmetry Axes	10	2	261	12
Transistor Pairs	19	6	6,218	186
Additional Symmetry Constraints	132	42	41,943	1,302
Runtime on Solving Symmetry Constraints	0.65 s	0.26 s	2 hr 36 min	48 min
Total Runtime for Retargeting Tool	10.06 s	9.31 s	4 hr 20 min	2 hr 14 min

listed in same row or column. During resizing, these unnecessary symmetric-pairs resulted in the increase of symmetry constraints from 1,302 to 41,943, which subsequently increased the runtime of solving the symmetry constraints from 48 minutes to 156 minutes. The overall runtime escalated from about 2 hours to 4 hours. Nevertheless, both target layouts showed similar symmetries and matching. The original layout had an area of 12,780 um². The target layout from direct symmetry detection had an area of 7,955 um². And the target layout for hierarchical symmetry detection had an area of 6,984 um². The reduction in area is attributed to the avoidance of unwanted axes of symmetry that constrain the layout. The retargeted layout obtained through HiLSD method is shown in Fig. 10.
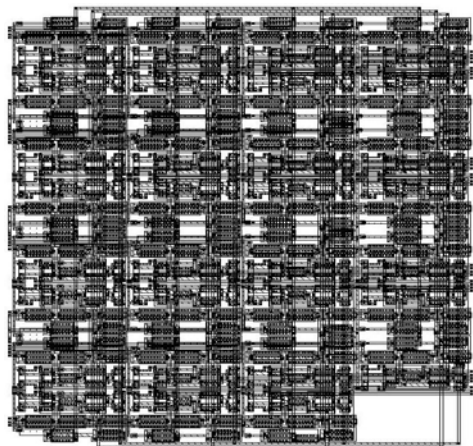

Fig. 10: Retargeted Layout of comparator block of ADC in TSMC 0.18um (HiLSD based symmetry detection).

Table 6: Comparison of a latched-comparator performance

Design Specs.	Layout in 0.25um	Retargeted Layout in 0.18um	
	-	DLSD Based	HiLSD Based
Power Supply	2.5 V	1.8 V	1.8 V
Ref. Voltage	1.28 V	1.28 V	1.28 V
Frequency	500 MHz	750 MHz	750 MHz
Resolution	20 mV	20 mV	20 mV
Area	369 um²	225 um²	214 um²
Power	0.84 mW	0.45 mW	0.45 mW

VII. Conclusions

A new symmetry detection tool, Hi-LSD, based on hierarchical extraction and subcircuit specific symmetric transistor pairs is presented. The tool significantly reduces search-space and ignores all unintended symmetry axes exhibited on the layout. Employing Hi-LSD on a 5-bit flash analog-to-digital converter ignores all unintended axes of symmetry and reduces the number of symmetric pairs from 6,218 to 186. When applied with the automatic analog

layout-retargeting tool, the runtime for regenerating the new ADC layout is reduced from 4 hours to 2 hours.

With the symmetry constraints described in a hierarchical circuit netlist by circuit designers, Hi-LSD also provides the first automatic tool for verifying if a layout meets all the symmetry constraints required by circuit designers.

Acknowledgements

References

[1] M. J. M. Pelgrom, A. C. J. Duinmaijer and A. P. G. Welbers, "Matching properties of MOS transistors", *IEEE J. Solid-State Circuits*, vol. 24, pp. 1433-1440, Oct. 1989.

[2] B. Razavi, *Design of Analog CMOS Integrated Circuits*, McGraw Hill, 2001.

[3] A. Hastings, *The Art of Analog Layout,* Prentice Hall, 2001.

[4] J. M. Cohn, D.J. Garrod, R. A. Rutenbar and L. R. Carley, "KOAN/ANAGRAM II: New tools for device-level analog placement and routing", *IEEE J. Solid State Circuits*, vol. 26, pp. 330-342, Mar. 1991.

[5] K. Lampaert, G. Gielen and W. M. Sansen, "A performance-driven placement tool for analog integrated circuits", *IEEE J. Solid State Circuits*, vol. 30, pp. 773-780, Jul. 1995.

[6] J. D. Conway and G. G. Schrooten, "An automatic layout generator for analog circuits", *Proc. European Design Automation Conference,* pp. 513-519, Mar. 1992.

[7] R. Castro-Lopez, F. V. Fernandez, F. Medeiro and A. Rodriguez-Vazquez, "Generation of technology-independent retargetable analog blocks", *Int. J. Analog Integrated Circuits and Signal Processing,* vol. 33, pp. 157-170, Dec. 2002.

[8] N. Jangkrajarng, S. Bhattacharya, R. Hartono, and C-J. R. Shi, "Automatic analog layout retargeting for new processes and device sizes", *Proc. IEEE Int. Symposium Circuits and Systems*, vol. 4, pp. 704-707, May 2003.

[9] R. Okuda, T. Sato, H. Onodera and K. Tamaru, "An efficient algorithm for layout compaction problem with symmetry constraints", *Proc. Int. Conference Computer-Aided-Design*, pp. 148-151, Nov. 1989.

[10] Y. Bourai and C. J. R. Shi, "Symmetry detection for automatic analog layout recycling", *Proc. Asian and South Pacific Design Automation Conference,* pp. 5-8, Jan. 1999.

[11] W. S. Scott and J. K. Ousterhout, "Magic's circuit extractor", *Proc. IEEE/ACM Design Automation Conference*, pp. 286-292, Jun. 1985.

[12] M. Ohlrich, C. Ebeling, E. Ginting and L. Sather, "Subgemini: Identifying subcircuits using a fast subgraph isomorphism algorithm", *Proc. IEEE/ACM Design Automation Conference,* pp. 31-37, Jun. 1993.

[13] S. L. Lin and J. Allen, "Minplex – a compactor that minimizes the bounding rectangle and individual rectangles in a layout", *Proc. IEEE/ACM Design Automation Conference*, pp. 123-130, Jun. 1986.

[14] D. Luenberger, *Linear and Nonlinear Programming* 2nd Edition, Addison-Wesley, 1984.